Dyes and Pigments 86 (2010) 249–258

Contents lists available at ScienceDirect

Dyes and Pigments

journal homepage: www.elsevier.com/locate/dyepig

The synthesis and optical properties of novel 1,3,4-oxadiazole derivatives containing an imidazole unit

Yun-Nan Yan, Wen-long Pan, Hua-Can Song*

School of Chemistry and Chemical Engineering, Sun Yat-Sen University, Guangzhou 510275, China

ARTICLE INFO

Article history:
Received 3 September 2009
Received in revised form
19 January 2010
Accepted 20 January 2010
Available online 10 February 2010

Keywords:
Synthesis
Fluorescence
Optical property
Crystal structure
1,3,4-Oxadiazoles
Imidazole

ABSTRACT

A series of 1,3,4-oxadiazole derivatives containing an imidazole unit were synthesized and characterized using ^{1}H NMR, ^{13}C NMR, mass spectrometry (or high-resolution mass spectrometry) and elemental analysis. The crystal structure of 2,5-bis(4-(1-*n*-butyl-4,5-diphenylimidazol-2-yl)phenyl)-1,3,4-oxadiazole was determined as monoclinic, space group C2/c type, using single crystal X-ray crystallography. For nine samples, UV–visible absorption coefficient (ε), maximum wavelength (λ_{max}), fluorescence excitation wavelength (λ_{ex}), fluorescence emission wavelength (λ_{em}), fluorescence quantum yield (Φ_F), fluorescence lifetime (T) were measured in dichloromethane and in the solid state. For these selected compounds, thermogravimetric analysis was also employed and structure:optical behaviour characteristics were discussed.

1. Introduction

Imidazole derivatives are important five-membered nitrogen-containing heterocyclic compounds which are widely used in many fields, such as P38 MAP kinase [1], antivascular disrupting, anti-tumour activator [2], ionic liquids [3], anion sensors [4], as well as electrical and optical materials [5–7]. 1,3,4-Oxadiazoles are a class of significant heterocyclic compounds used in medicinal and pesticide chemistry [8,9], asymmetric organic synthesis [10], and polymer and materials science [11,12]. 2,5-Diaryl-1,3,4-oxadiazoles are important materials used as red luminescent emitters with carrier-transporting ability [13], efficient electron transporting and hole blocking materials in organic light-emitting diodes (OLEDs) [14–28].

The work described by the current authors relates to the synthesis and optical properties of heterocycle-based chromophores [29–31]. There are a few reports of the synthesis and optical properties of such compounds that contain 1,3,4-oxadiazole and imidazole or benzoimidazole units within a conjugated, long chain molecule [28,32]. Hence, novel fluorescent dyes using a benzene ring to link an aryl-1,3,4-oxadiazole unit and arylimidazole unit or benzoimidazole unit were prepared so as to investigate their UV–visible absorption and fluorescence character. The synthetic pathway and the structures of the target molecules are shown in Figs. 1 and 2.

2. Experimental

2.1. Reagents and instruments

All melting points were determined on an X4 melting point microscope. ^{1}H NMR and ^{13}C NMR spectra were measured on a Bruker AVANCE-300 NMR spectrometer. MS were taken with an SHIMADZU LCMS-2010A. High-resolution mass spectra were obtained on Thermo MAT-95XP. Element analyses were taken with an Elementar Analysensysteme GmbH Vario EL. Single crystal was characterized by Bruker Smart 1000 CCD X-ray single crystal diffractometer. Ultraviolet and fluorescence spectra were recorded on an SHIMADZU UV-1601 and SHIMADZU RF-5301PC spectrofluorophotometer. Fluorescence lifetimes were determined on EDINBURGH FLSP920. Thermogravimetric analysis (TGA) was carried out up to 900 °C with a heating speed of 10.0 K/min in nitrogen atmosphere on a Netzsch TG-209 thermogravimetric analyzer. Reagents and solvents used for the synthesis were all synthetic grades and used without further purification.

* Corresponding author. Tel.: +86 20 84110918; fax: +86 20 84112245.
E-mail address: yjhxhc@mail.sysu.edu.cn (H.-C. Song).

0143-7208/$ – see front matter © 2010 Elsevier Ltd. All rights reserved.
doi:10.1016/j.dyepig.2010.01.011

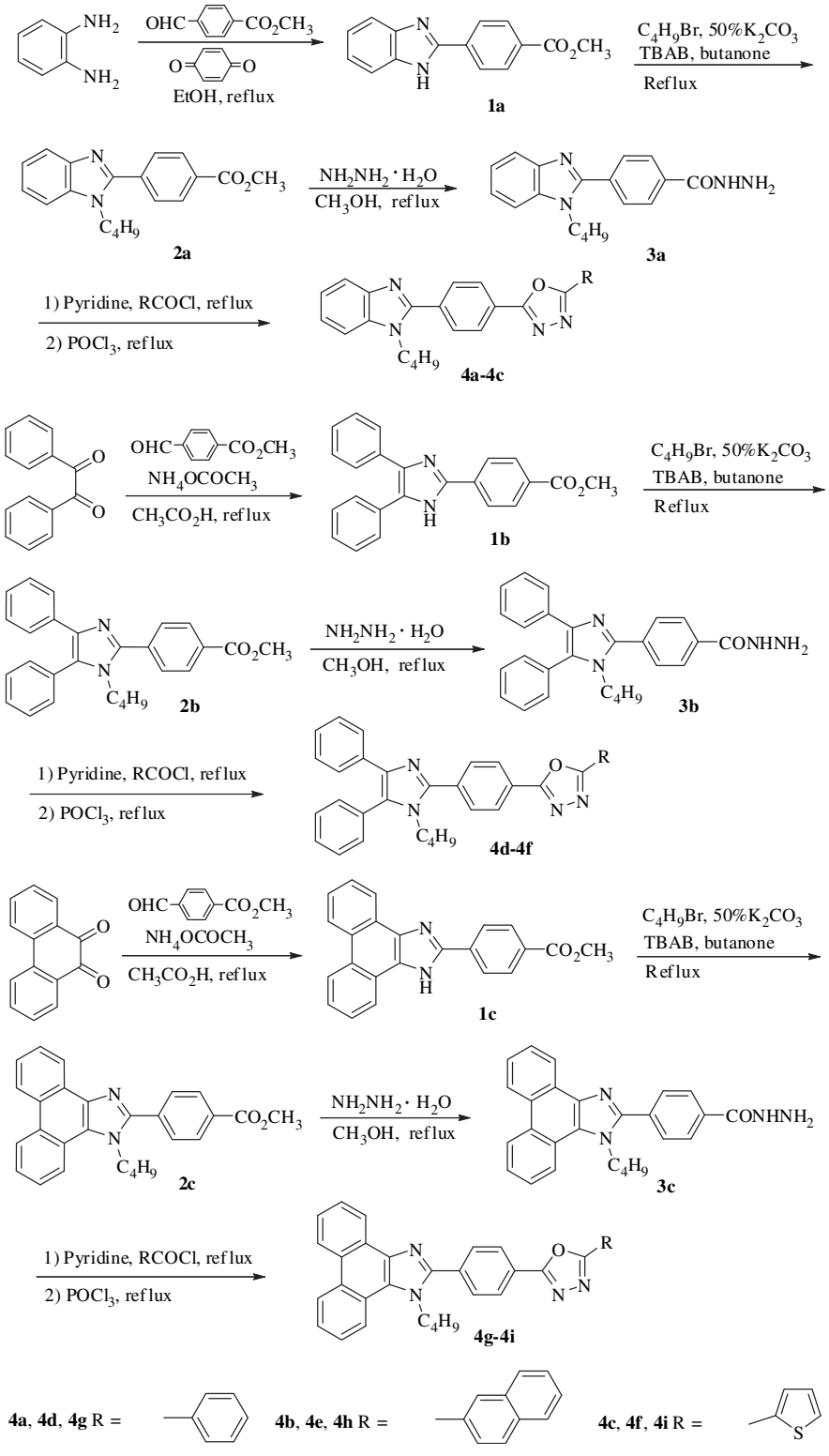

Fig. 1. The synthetic route of unsymmetrical 1,3,4-oxadiazole derivatives.

2.2. Synthesis

2.2.1. Preparation of ***1a–c***

Compound **1a** was prepared according to the reported method [33], while compounds **1b** and **1c** were obtained using reported procedures [34].

*2.2.1.1. Methyl 4-(1H-benzimidazol-2-yl)benzoate (**1a**).* White solid, yield 50%; m.p. 220–221 °C (Lit. [35] 220–221 °C). ^{1}H NMR (300 MHz, DMSO-d_6): δ 3.89 (s, 3H, OCH_3), 7.18–7.27 (m, 2H, ArH), 7.56 (d, J = 7.5 Hz, 1H, ArH), 7.70 (d, J = 7.2 Hz, 1H, ArH), 8.12 (d, J = 8.4 Hz, 2H, ArH), 8.31 (d, J = 8.4 Hz, 2H, ArH), 13.10 (s, 1H, NH). ^{13}C NMR (75 MHz, DMSO-d_6): δ 52.2,

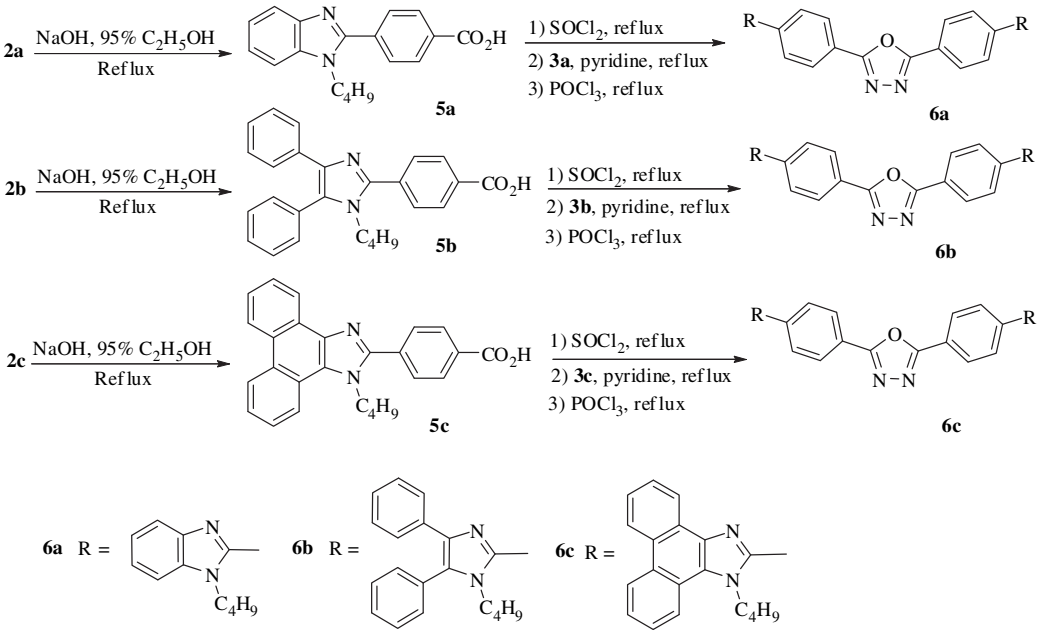

Fig. 2. The synthetic scheme of symmetrical 1,3,4-oxadiazole derivatives.

126.4, 129.6, 130.1, 134.1, 149.8, 165.5. ESI-MS (*m*/*z*): 253 $[M + H]^+$.

*2.2.1.2. Methyl 4-(4,5-diphenylimidazol-2-yl)benzoate (**1b**).* Yellowish solid, yield 93%; m.p. 235–236 °C (Lit. [36] 246–248 °C). ^{1}H NMR (300 MHz, DMSO-d_6): δ 3.88 (s, 3H, OCH_3), 7.19–7.35 (m, 3H, ArH), 7.38–7.59 (m, 7H, ArH), 8.06 (d, J = 8.4 Hz, 2H, ArH), 8.23 (d, J = 8.1 Hz, 2H, ArH), 12.93 (s, 1H, NH). ESI-MS (*m*/*z*): 355 $[M + H]^+$.

*2.2.1.3. Methyl 4-(1H-phenanthroimidazol-2-yl)benzoate (**1c**).* Yellowish solid, yield 90%; m.p. >300 °C. ^{1}H NMR (300 MHz, DMSO-d_6): δ 3.89 (s, 3H, OCH_3), 7.54–7.76 (m, 4H, ArH), 8.12 (s, 2H, ArH), 8.41 (s, 2H, ArH), 8.51 (s, 1H, ArH), 8.61 (d, J = 7.5 Hz, 1H, ArH), 8.66–8.87 (m, 2H, ArH), 13.51 (s, 1H, NH). ESI-MS (*m*/*z*): 353 $[M + H]^+$.

*2.2.2. General procedure for the synthesis of **2a–c***

A mixture of methyl 4-(imidazol-2-yl)benzoate derivative (2.5 mmol), *n*-butyl bromide (3.5 mmol), tetra-*n*-butylammonium bromide (TBAB) (0.25 g), 50% potassium carbonate (10 mL) and butanone (10 mL) was refluxed for 20–24 h and the reaction was monitored by TLC. After butanone was removed, the residue was poured into water (100 mL). The solid was collected and purified by silica-gel column chromatography to offer the corresponding product.

*2.2.2.1. Methyl 4-(1-n-butylbenzimidazol-2-yl)benzoate (**2a**).* White solid, yield 75%; m.p. 100–101 °C. ^{1}H NMR (300 MHz, DMSO-d_6): δ 0.74 (t, J = 7.2 Hz, 3H, CH_3), 1.07–1.19 (m, 2H, CH_2), 1.59–1.72 (m, 2H, CH_2), 3.91 (s, 3H, OCH_3), 4.33 (t, J = 6.7 Hz, 2H, NCH_2), 7.22–7.33 (m, 2H, ArH), 7.68 (t, J = 7.5 Hz, 2H, ArH), 7.94 (d, J = 7.5 Hz, 2H, ArH), 8.14 (d, J = 7.5 Hz, 2H, ArH). ^{13}C NMR (75 MHz, DMSO-d_6): δ 13.1, 19.1, 31.1, 43.7, 52.1, 110.7, 119.1, 121.8, 122.5, 129.1, 129.2, 130.0, 134.7, 135.5, 142.3, 151.4, 165.4. ESI-MS (*m*/*z*): 309 $[M + H]^+$.

*2.2.2.2. Methyl 4-(1-n-butyl-4,5-diphenylimidazol-2-yl)benzoate (**2b**).* Yellowish solid, yield 70%; m.p. 134–135 °C. ^{1}H NMR (300 MHz, DMSO-d_6): δ 0.52 (t, J = 7.2 Hz, 3H, CH_3), 0.84–0.96 (m, 2H, CH_2), 1.20–1.32 (m, 2H, CH_2), 3.89 (s, 3H, OCH_3), 3.94 (t, J = 7.2 Hz, 2H, NCH_2), 7.09–7.21(m, 3H, ArH), 7.37–7.49 (m, 4H, ArH), 7.50–7.57 (m, 3H, ArH), 7.90 (d, J = 8.4 Hz, 2H, ArH), 8.11 (d, J = 8.4 Hz, 2H, ArH). ^{13}C NMR (75 MHz, DMSO-d_6, δ ppm): 13.0, 18.8, 31.7, 44.1, 52.2, 126.0, 126.2, 127.9, 128.6, 128.8, 128.9, 129.0, 129.2, 129.3, 130.5, 130.7, 134.2, 135.3, 136.9, 145.3, 165.7. ESI-MS (*m*/*z*): 411 $[M + H]^+$.

*2.2.2.3. Methyl 4-(1-n-butylphenanthroimidazol-2-yl)benzoate (**2c**).* Yellowish solid, yield 74%; m.p. 101–102 °C. ^{1}H NMR (300 MHz, $CDCl_3$): δ 0.82 (t, J = 7.2 Hz, 3H, CH_3), 1.18–1.31 (m, 2H, CH_2), 1.88–1.97 (m, 2H, CH_2), 4.00 (s, 3H, OCH_3), 4.64 (t, J = 7.2 Hz, 2H, NCH_2), 7.61–7.73 (m, 4H, ArH), 7.87 (d, J = 8.7 Hz, 2H, ArH), 8.22–8.28 (m, 3H, ArH), 8.72 (d, J = 7.8 Hz, 1H, ArH), 8.79 (dd, J = 1.5 Hz, 7.8 Hz, 1H, ArH), 8.86 (dd, J = 1.8 Hz, 7.8 Hz, 1H, ArH). ESI-MS (*m*/*z*): 409 $[M + H]^+$.

*2.2.3. General procedure for the preparation of **3a–c***

A mixture of methyl benzoate derivatives (5 mmol), hydrazine hydrate (15 mmol), and methanol (15 mL) was refluxed for 12 h. The reaction was monitored by TLC. After the solvent was removed, the residue was thoroughly washed with water and dried completely to give pure product.

*2.2.3.1. 4-(1-n-Butylbenzimidazol-2-yl)benzohydrazide (**3a**).* White solid, yield 80%; m.p. 62 °C. ^{1}H NMR (300 MHz, DMSO-d_6): δ 0.75 (t, J = 7.2 Hz, 3H, CH_3), 1.06–1.19 (m, 2H, CH_2), 1.59–1.69 (m, 2H, CH_2), 4.32 (t, J = 6.6 Hz, 2H, NCH_2), 4.59 (s, 2H, NH_2), 7.21–7.34 (m, 2H, ArH), 7.67 (t, J = 7.2 Hz, 2H, ArH), 7.85 (d, J = 8.1 Hz, 2H, ArH), 8.00 (d, J = 7.8 Hz, 2H, ArH), 9.93 (s, 1H, NH). ^{13}C NMR (75 MHz, DMSO-d_6): δ 13.2, 19.2, 31.2, 43.8, 110.8, 119.1, 121.9, 122.4, 127.2, 128.9, 132.8, 133.9, 135.5, 142.4, 151.9, 165.0. ESI-MS (*m*/*z*): 309 $[M + H]^+$.

*2.2.3.2. 4-(1-n-Butyl-4,5-diphenylimidazol-2-yl)benzohydrazide (**3b**).* Yellowish solid, yield 78%; m.p. 193–194 °C. ^{1}H NMR (300 MHz, DMSO-d_6): δ 0.53 (t, J = 7.2 Hz, 3H, CH_3), 0.85–0.97 (m, 2H, CH_2), 1.21–1.31 (m, 2H, CH_2), 3.93 (t, J = 7.2 Hz, 2H, NCH_2), 7.09–7.21 (m, 3H, ArH), 7.39–7.55 (m, 7H, ArH), 7.84 (d, J = 8.1 Hz, 2H, ArH), 7.98 (d, J = 8.1 Hz, 2H, ArH). ESI-MS (*m*/*z*): 411 $[M + H]^+$.

*2.2.3.3. 4-(1-n-Butylphenanthroimidazol-2-yl)benzohydrazide (**3c**).* White solid, yield 80%; m.p. 223–224 °C. ^{1}H NMR (300 MHz, DMSO-d_6): δ 0.69 (t, J = 7.2 Hz, 3H, CH_3), 1.03–1.18 (m, 2H, CH_2), 1.73–1.87 (m, 2H, CH_2), 4.57 (t, J = 7.5 Hz, 2H, NCH_2), 4.69 (br, 2H, NH_2), 7.58–7.81 (m, 4H, ArH), 7.87 (d, J = 6.9 Hz, 2H, ArH), 8.06 (d, J = 7.8 Hz, 2H, ArH), 8.33–8.44 (m, 1H, ArH), 8.59 (d, J = 7.5 Hz, 1H, ArH), 8.77–8.88 (m, 1H, ArH), 8.89–9.00 (m, 1H, ArH), 9.96 (s, 1H, CONH). ESI-MS (m/z): 409 $[M + H]^+$.

*2.2.4. General procedure for the synthesis of **4a–i***

The benzohydrazide derivative (2 mmol) was added to a stirred solution of the corresponding benzoyl chloride (or 2-naphthoyl chloride, or thiophene-2-carbonyl chloride) (2 mmol) in anhydrous pyridine (10 mL). The mixture was refluxed for 20–24 h, cooled and washed with water and the ensuing crude product was filtered, dried and then was added to phosphorus oxychloride (caution: reacts violently with water; incompatible with many metals, alcohols, amines, phenol, DMSO, strong bases; 10 mL); the mixture was refluxed overnight. The majority of phosphorus oxychloride was distilled from the reaction mixture and the residue was gently added to powdered ice. The resulting oxadiazole product was filtered, washed with water, dried and recrystallized from the mixture of chloroform and ethanol, or purified by silica-gel column chromatography using petroleum (b.p. 60–90 °C)/ethyl acetate (2:1) as eluent.

*2.2.4.1. 2-(4-(1-**n**-Butylbenzimidazol-2-yl)phenyl)-5-phenyl-1,3,4-oxadiazole (**4a**).* White solid, yield 50%; m.p. 144–146 °C. ^{1}H NMR (300 MHz, DMSO-d_6): δ 0.77 (t, J = 7.2 Hz, 3H, CH_3), 1.11–1.23 (m, 2H, CH_2), 1.64–1.74 (m, 2H, CH_2), 4.38 (t, J = 6.9 Hz, 2H, NCH_2), 7.24–7.34 (m, 2H, ArH), 7.64–7.73 (m, 5H, ArH), 8.06 (d, J = 8.1 Hz, 2H, ArH), 8.17 (d, J = 7.5 Hz, 2H, ArH), 8.33 (d, J = 8.1 Hz, 2H, ArH). ^{13}C NMR (75 MHz, DMSO-d_6): δ 13.3, 19.2, 31.2, 43.9, 110.9, 119.1, 122.0, 122.6, 123.1, 123.9, 126.6, 126.8, 129.2, 129.8, 131.9, 133.4, 135.6, 142.2, 151.3, 163.3, 163.9. ESI-MS (m/z): 395 $[M + H]^+$. Anal. Calcd. (%) for $C_{25}H_{22}N_4O\cdot1.5H_2O$: C, 71.24; H, 5.98; N, 13.29. Found: C, 71.40; H, 5.80; N, 13.39.

*2.2.4.2. 2-(4-(1-n-Butylbenzimidazol-2-yl)phenyl)-5-(naphthalen-2-yl)-1,3,4-oxadiazole (**4b**).* White solid, yield 46%; m.p. 216–218 °C. ^{1}H NMR (300 MHz, DMSO-d_6): δ 0.79 (t, J = 7.2 Hz, 3H, CH_3), 1.13–1.25 (m, 2H, CH_2), 1.66–1.75 (m, 2H, CH_2), 4.39 (t, J = 7.2 Hz, 2H, NCH_2), 7.25–7.35 (m, 2H, ArH), 7.65–7.73 (m, 5H, ArH), 8.03–8.08 (m, 3H, ArH), 8.14–8.23 (m, 3H, ArH), 8.38 (d, J = 8.1 Hz, 2H, ArH), 8.80 (s, 1H, ArH). ^{13}C NMR (75 MHz, $CDCl_3$): δ 13.6, 20.0, 31.9, 44.7, 110.1, 120.0, 120.8, 122.5, 123.0, 123.1, 124.7, 127.0, 127.1, 127.3, 127.8, 127.9, 128.7, 128.9, 129.8, 132.7, 133.7, 134.6, 135.6, 142.9, 152.0, 163.9, 164.8. ESI-MS (m/z): 445 $[M + H]^+$. Anal. Calcd. (%) for $C_{29}H_{24}N_4O\cdot0.4H_2O$: C, 77.11; H, 5.53; N, 12.40. Found: C, 77.03; H, 5.40; N, 12.30.

*2.2.4.3. 2-(4-(1-n-Butylbenzimidazol-2-yl)phenyl)-5-(thiophen-2-yl)-1,3,4-oxadiazole (**4c**).* White solid, yield 45%; m.p. 111–112 °C. ^{1}H NMR (300 MHz, DMSO-d_6): δ 0.77 (t, J = 7.2 Hz, 3H, CH_3), 1.10–1.23 (m, 2H, CH_2), 1.64–1.73 (m, 2H, CH_2), 4.38 (t, J = 7.2 Hz, 2H, NCH_2), 7.23–7.36 (m, 3H, ArH), 7.70 (t, J = 7.2 Hz, 2H, ArH), 7.99–8.01 (m, 2H, ArH), 8.05 (d, J = 8.7 Hz, 2H, ArH), 8.28 (d, J = 8.7 Hz, 2H, ArH). ^{13}C NMR (75 MHz, DMSO-d_6): δ 13.3, 19.2, 31.3, 43.9, 110.9, 119.2, 122.0, 122.6, 122.7, 123.7, 124.0, 126.8, 128.6, 129.9, 130.6, 131.7, 133.4, 135.6, 142.3, 151.4, 160.4, 162.8. ESI-MS (m/z): 401 $[M + H]^+$. Anal. Calcd. (%) for $C_{23}H_{20}N_4OS\cdot1\cdot1H_2O$: C, 65.72; H, 5.32; N, 13.33. Found: C, 65.50; H, 5.25; N, 13.29.

*2.2.4.4. 2-(4-(1-n-Butyl-4,5-diphenylimidazol-2-yl)phenyl)-5-phenyl-1,3,4-oxadiazole (**4d**).* Yellowish solid, yield 45%; m.p. 147–148 °C. ^{1}H NMR (300 MHz, $CDCl_3$): δ 0.64 (t, J = 7.5 Hz, 3H, CH_3), 0.98–1.05 (m, 2H, CH_2), 1.32–1.43 (m, 2H, CH_2), 3.96 (t, J = 6.9 Hz, 2H, NCH_2), 7.10–7.24 (m, 4H, ArH), 7.42–7.55 (m, 9H, ArH), 7.92 (d, J = 8.1 Hz, 2H, ArH), 8.11–8.20 (m, 2H, ArH), 8.27 (d, J = 7.2 Hz, 2H, ArH). ^{13}C NMR (75 MHz, $CDCl_3$): δ 13.4, 19.6, 32.7, 44.8, 123.8, 126.3, 126.7, 126.9, 127.0, 127.9, 128.7, 128.9, 129.4, 130.4, 130.9, 131.1, 131.7, 134.2, 134.6, 138.2, 146.1, 164.1, 164.6. HRMS (EI) (M^+): Calcd. for $C_{33}H_{28}N_4O$: 496.2263; found: 496.2258. Anal. Calcd. (%) for $C_{33}H_{28}N_4O$: C, 79.81; H, 5.68; N, 11.28. Found: C, 79.61; H, 5.87; N, 11.33.

*2.2.4.5. 2-(4-(1-n-Butyl-4,5-diphenylimidazol-2-yl)phenyl)-5-(naphthalen-2-yl)-1,3,4-oxadiazole (**4e**).* White solid, yield 44%; m.p. 206–208 °C. ^{1}H NMR (300 MHz, DMSO-d_6): δ 0.57 (t, J = 7.2 Hz, 3H, CH_3), 0.90–1.02 (m, 2H, CH_2), 1.28–1.38 (m, 2H, CH_2), 4.01 (t, J = 7.5 Hz, 2H, NCH_2), 7.11–7.24 (m, 3H, ArH), 7.41–7.60 (m, 7H, ArH), 7.60–7.72 (m, 2H, ArH), 8.02–8.07 (m, 3H, ArH), 8.15–8.24 (m, 3H, ArH), 8.36 (d, J = 8.7 Hz, 2H, ArH), 8.82 (s, 1H, ArH). ^{13}C NMR (75 MHz, $CDCl_3$): δ 13.4, 19.6, 32.7, 44.8, 121.0, 123.2, 123.8, 126.3, 126.7, 127.0, 127.1, 127.3, 127.8, 127.9, 128.0, 128.7, 128.8, 129.0, 129.5, 130.5, 130.9, 131.1, 132.8, 134.2, 134.6, 138.3, 146.1, 164.2, 164.8. ESI-MS (m/z): 547 $[M + H]^+$. Anal. Calcd. (%) for $C_{37}H_{30}N_4O\cdot0.2H_2O$: C, 80.76; H, 5.57; N, 10.18. Found: C, 80.77; H, 5.59; N, 10.21.

*2.2.4.6. 2-(4-(1-n-Butyl-4,5-diphenylimidazol-2-yl)phenyl)-5-(thiophen-2-yl)-1,3,4-oxadiazole (**4f**).* Yellowish solid, yield 41%; m.p. 168–169 °C. ^{1}H NMR (300 MHz, $CDCl_3$): δ 0.60 (t, J = 6.9 Hz, 3H, CH_3), 0.90–1.06 (m, 2H, CH_2), 1.23–1.40 (m, 2H, CH_2), 4.09 (t, J = 7.2 Hz, 2H, NCH_2), 7.14–7.32 (m, 4H, ArH), 7.33–7.48 (m, 4H, ArH), 7.49–7.62 (m, 4H, ArH), 7.85 (s, 1H, ArH), 8.01 (d, J = 7.2 Hz, 2H, ArH), 8.28 (d, J = 7.2 Hz, 2H, ArH). ^{13}C NMR (75 MHz, $CDCl_3$): δ 13.3, 19.5, 32.6, 44.8, 123.5, 124.9, 126.3, 126.7, 127.0, 127.9, 128.1, 128.7, 128.9, 129.4, 129.8, 130.2, 130.4, 130.8, 131.0, 134.2, 134.6, 138.2, 146.0, 160.8, 163.5. ESI-MS (m/z): 503 $[M + H]^+$. Anal. Calcd. (%) for $C_{31}H_{26}N_4OS$: C, 74.08; H,5.21; N, 11.15. Found: C, 73.83; H, 5.27; N, 11.19.

*2.2.4.7. 2-(4-(1-n-Butylphenanthroimidazol-2-yl)phenyl)-5-phenyl-1,3,4-oxadiazole (**4g**).* Yellowish solid, yield 40%; m.p. 209–210 °C. ^{1}H NMR (300 MHz, $CDCl_3$): δ 0.85 (t, J = 6.6 Hz, 3H, CH_3), 1.19–1.36 (m, 2H, CH_2), 1.90–2.07 (m, 2H, CH_2), 4.70 (t, J = 6.9 Hz, 2H, NCH_2), 7.51–7.61 (m, 3H, ArH), 7.61–7.77 (m, 4H, ArH), 7.99 (d, J = 7.8 Hz, 2H, ArH), 8.12–8.30 (m, 3H, ArH), 8.37 (d, J = 7.8 Hz, 2H, ArH), 8.72 (d, J = 8.1 Hz, 1H, ArH), 8.76–8.91 (m, 2H, ArH). ^{13}C NMR (75 MHz, $CDCl_3$): δ 13.5, 19.6, 29.7, 46.9, 120.6, 122.4, 122.9, 123.2, 123.6, 124.3, 124.8, 125.5, 126.4, 126.7, 126.8, 126.9, 127.1, 127.2, 128.1, 128.9, 129.1, 130.5, 131.7, 134.0, 138.1, 151.1, 163.8, 164.6. HRMS (EI) (M^+): Calcd. for $C_{33}H_{26}N_4O$: 494.2107; found: 494.2102. Anal. Calcd. (%) for $C_{33}H_{26}N_4O\cdot0.5H_2O$: C, 78.99; H, 5.38; N, 11.17. Found: C, 78.93; H, 6.06; N, 10.98.

*2.2.4.8. 2-(4-(1-n-Butylphenanthroimidazol-2-yl)phenyl)-5-(naphthalen-2-yl)-1,3,4-oxadiazole (**4h**).* Yellowish solid, yield 34%; m.p. 259–260 °C. ^{1}H NMR (300 MHz, $CDCl_3$): δ 0.86 (t, J = 7.2 Hz, 3H, CH_3), 1.23–1.35 (m, 2H, CH_2), 1.90–2.03 (m, 2H, CH_2), 4.69 (t, J = 7.2 Hz, 2H, NCH_2), 7.58–7.75 (m, 6H, ArH), 7.91–7.94 (m, 1H, ArH), 7.99 (t, J = 9.0 Hz, 4H, ArH), 8.27 (t, J = 8.7 Hz, 2H, ArH), 8.40 (d, J = 8.1 Hz, 2H, ArH), 8.67–8.72 (m, 2H, ArH), 8.81 (d, J = 7.2 Hz, 1H, ArH), 8.86 (d, J = 7.8 Hz, 1H, ArH). ^{13}C NMR (75 MHz, $CDCl_3$): δ 13.2, 19.3, 30.9, 48.9, 120.2, 120.6, 121.9, 122.2, 122.6, 123.9, 124.2, 124.3, 124.8, 126.7, 126.8, 126.9, 126.9, 126.9, 127.1, 127.6, 127.7, 127.8, 128.3, 128.7, 129.6, 132.1, 132.4, 134.5, 146.5, 162.7, 164.7. ESI-MS (m/z): 545 $[M + H]^+$. Anal. Calcd. (%) for $C_{37}H_{28}N_4O\cdot0.7H_2O$: C, 79.75; H, 5.32; N, 10.05. Found: C, 79.72; H, 5.42; N 9.72.

*2.2.4.9. 2-(4-(1-n-Butylphenanthroimidazol-2-yl)phenyl)-5-(thiophen-2-yl)-1,3,4-oxadiazole (**4i**).* Yellowish solid, yield 35%; m.p. 231–232 °C. ^{1}H NMR (300 MHz, $CDCl_3$): δ 0.63 (t, J = 7.5 Hz, 3H, CH_3), 0.93–1.05 (m, 2H, CH_2), 1.73–1.82 (m, 2H, CH_2), 5.06 (t, J = 6.9 Hz, 2H, NCH_2), 7.17–7.23 (m, 1H, ArH), 7.24–7.29 (m, 1H, ArH), 7.40 (t, J = 7.8 Hz, 1H, ArH), 7.56–7.82 (m, 4H, ArH), 8.09 (d, J = 8.1 Hz, 2H, ArH), 8.28 (d, J = 8.1 Hz, 1H, ArH), 8.36 (t, J = 8.4 Hz, 3H, ArH), 8.49 (d, J = 8.1 Hz, 1H, ArH), 8.91 (d, J = 7.8 Hz, 1H, ArH). ^{13}C NMR (75 MHz, $CDCl_3$): δ 13.2, 19.3, 31.0, 48.9, 119.6, 120.6, 121.9, 122.3, 124.1, 124.3, 124.4, 124.8, 126.5, 127.0, 127.1, 127.8, 127.9, 128.2, 128.5, 129.7, 130.2, 130.6, 132.0, 146.4, 160.9, 162.0. ESI-MS (m/z): 501 $[M + H]^+$. Anal. Calcd. (%) for $C_{31}H_{24}N_4OS\cdot 0.4H_2O$: C, 73.32; H, 4.92; N 11.03. Found: C, 73.76; H, 4.96; N, 10.90.

*2.2.5. General procedure for the synthesis of **5a**–**c***

The mixture of corresponding compound **2** (5 mmol) and sodium hydroxide (10 mmol) in 95% methanol (10 mL) was refluxed for about 1 h. After most solvent was evaporated, the residue was dissolved in water (20 mL), the pH was adjusted to 1.0 with concentrated hydrochloric acid, and then the resulting solid was filtered, washed, and dried to give pure **5a**, **5b** and **5c**.

*2.2.5.1. 4-(1-n-Butylbenzimidazol-2-yl)benzoic acid (**5a**).* White solid, yield 75%; m.p. 235–236 °C. ^{1}H NMR (300 MHz, DMSO-d_6): δ 0.76 (t, J = 7.2 Hz, 3H, CH_3), 1.11–1.23 (m, 2H, CH_2), 1.65–1.75 (m, 2H, CH_2), 4.40 (t, J = 7.2 Hz, 2H, NCH_2), 7.42–7.51 (m, 2H, ArH), 7.81 (d, J = 7.8 Hz, 1H, ArH), 7.91 (t, J = 7.5 Hz, 1H, ArH), 7.99 (d, J = 7.8 Hz, 2H, ArH), 13.39 (s, 1H, COOH). ESI-MS (m/z): 293 $[M - H]^-$.

*2.2.5.2. 4-(1-n-Butyl-4,5-diphenylimidazol-2-yl)benzoic acid (**5b**).* Yellowish solid, yield 80%; m.p. 124–125 °C (lit. [30] 124–126 °C). ^{1}H NMR (300 MHz, DMSO-d_6): δ 0.53 (t, J = 7.5 Hz, 3H, CH_3), 0.85–0.97 (m, 2H, CH_2), 1.22–1.32 (m, 2H, CH_2), 3.94 (t, J = 7.5 Hz, 2H, NCH_2), 7.09–7.21 (m, 3H, ArH), 7.39–7.57 (m, 7H, ArH), 7.88 (t, J = 8.4 Hz, 2H, ArH), 8.09 (d, J = 8.1 Hz, 2H, ArH), 13.10 (s, 1H, COOH). ^{13}C NMR (75 MHz, DMSO-d_6): δ 12.9, 18.8, 31.6, 44.0, 125.9, 126.0, 127.8, 128.4, 128.7, 128.8, 128.9, 129.4, 130.3, 130.4, 130.5, 130.6, 134.1, 134.8, 136.7, 166.6. ESI-MS (m/z): 395 $[M - H]^-$.

*2.2.5.3. 4-(1-n-Butylphenanthrimidazol-2-yl)benzoic acid (**5c**).* Yellowish solid, yield 82%; m.p. 261–262 °C. ^{1}H NMR (300 MHz, DMSO-d_6): δ 0.67 (t, J = 7.5 Hz, 3H, CH_3), 1.05–1.11 (m, 2H, CH_2), 1.75–1.84 (m, 2H, CH_2), 4.70 (t, J = 6.6 Hz, 2H, NCH_2), 7.62–7.71 (m, 3H, ArH), 7.74–7.81 (m, 1H, ArH), 7.94 (d, J = 8.1 Hz, 2H, ArH), 8.18 (d, J = 7.8 Hz, 2H, ArH), 8.42 (d, J = 8.1 Hz, 1H, ArH), 8.59 (d, J = 7.8 Hz, 1H, ArH), 8.87 (d, J = 8.4 Hz, 1H, ArH), 8.98 (d, J = 8.1 Hz, 1H, ArH), 13.25 (s, 1H, COOH). ESI-MS (m/z): 393 $[M - H]^-$.

*2.2.6. General procedure for the synthesis of **6a**–**c***

Compound **5a** or **5b** or **5c** (2 mmol) was added to thionyl chloride (caution: reacts violently with water; incompatible with most common metals, strong reducing agents, strong bases, alcohols; 15 mL), and the mixture was refluxed for 4 h. After thionyl chloride was evaporated, compound **3** and anhydrous pyridine (5 mL) was added. The mixture was refluxed for 20–24 h, cooled and treated with water, and then the crude product completely precipitated. The crude product was filtered, dried completely and added to phosphorus oxychloride (10 mL), the mixture was refluxed overnight. Most of the phosphorus oxychloride was distilled from the reaction mixture, and the residue was gently added to powdered ice. The oxadiazole was filtered, washed with water, dried and recrystallized from the mixture of chloroform and ethanol, then purified by silica-gel column chromatography using petroleum (b.p. 60–90 °C)/ethyl acetate (2:1) as eluent.

*2.2.6.1. 2,5-Bis(4-(1-n-butylbenzimidazol-2-yl)phenyl)-1,3,4-oxadiazole (**6a**).* White solid, yield 10%; m.p. 213–215 °C. ^{1}H NMR (300 MHz, DMSO-d_6): δ 0.79 (t, J = 7.2 Hz, 6H, CH_3), 1.23–1.25 (m, 4H, CH_2), 1.66–1.75 (m, 4H, CH_2), 4.40 (t, J = 7.2 Hz, 4H, NCH_2), 7.24–7.35 (m, 4H, ArH), 7.71 (t, J = 7.5 Hz, 4H, ArH), 8.07 (d, J = 8.4 Hz, 4H, ArH), 8.36 (d, J = 8.4 Hz, 4H, ArH). ^{13}C NMR (75 MHz, $CDCl_3$): δ 13.6, 20.0, 31.9, 44.7, 110.1, 120.0, 122.6, 123.1, 124.5, 127.1, 129.9, 133.9, 135.6, 142.9, 151.9, 164.1. HRMS (EI) (M^+): Calcd. for $C_{36}H_{34}N_6O$: 566.2794; found: 566.2792. Anal. Calcd. (%) for $C_{36}H_{34}N_6O$: C, 76.30; H, 6.05; N, 14.83. Found: C, 76.13; H, 6.18; N, 14.97.

*2.2.6.2. 2,5-Bis(4-(1-n-butyl-4,5-diphenylimidazol-2-yl)phenyl)-1,3,4-oxadiazole (**6b**).* White solid, yield 12%; m.p. 217–219 °C. ^{1}H NMR (300 MHz, DMSO-d_6): δ 0.57 (t, J = 7.2 Hz, 6H, CH_3), 0.90–1.02 (m, 4H, CH_2), 1.27–1.37 (m, 4H, CH_2), 4.00 (t, J = 7.2 Hz, 4H, NCH_2), 7.11–7.23 (m, 6H, ArH), 7.42–7.51 (m, 8H, ArH), 7.53–7.59 (m, 6H, ArH), 8.04 (d, J = 8.4 Hz, 4H, ArH), 8.33 (d, J = 8.4 Hz, 4H, ArH). ^{13}C NMR (75 MHz, $CDCl_3$): δ 13.3, 19.5, 32.6, 44.8, 123.6, 126.3, 126.7, 127.1, 127.9, 128.7, 128.9, 129.4, 130.5, 130.8, 131.0, 134.2, 134.7, 138.2, 146.0, 164.2. ESI-MS (m/z): 771 $[M + H]^+$. Anal. Calcd. (%) for $C_{52}H_{46}N_6O\cdot 0.6H_2O$: C, 79.89; H, 6.09; N, 10.75. Found: C, 79.79; H, 6.37; N 10.29.

*2.2.6.3. 2,5-Bis(4-(1-n-butylphenanthroimidazol-2-yl)phenyl)-1,3,4-oxadiazole (**6c**).* Yellowish solid, yield 15%; m.p. > 300 °C. ^{1}H NMR (300 MHz, $CDCl_3$): δ 0.85 (t, J = 6.6 Hz, 6H, CH_3), 1.20–1.36 (m, 4H, CH_2), 1.89–2.06 (m, 4H, CH_2), 4.70 (t, J = 6.0 Hz, 4H, NCH_2), 7.59–7.76 (m, 8H, ArH), 8.00 (d, J = 7.5 Hz, 4H, ArH), 8.30 (d, J = 7.2 Hz, 2H, ArH), 8.39 (d, J = 7.5 Hz, 4H, ArH), 8.72 (d, J = 7.8 Hz, 2H, ArH), 8.80 (d, J = 7.2 Hz, 2H, ArH), 8.86 (d, J = 7.5 Hz, 2H, ArH). ^{13}C NMR (300 MHz, $CDCl_3$): δ 13.6, 19.7, 32.5, 47.1, 120.7, 122.5, 123.0, 123.3, 124.3, 124.4, 124.9, 125.6, 126.5, 126.8, 127.2, 127.3, 128.2, 129.3, 130.7, 134.4, 138.3, 151.2, 164.3. ESI-MS (m/z): 768 $[M + H]^+$. Anal. Calcd. (%) for $C_{52}H_{42}N_6O$: C, 81.44; H, 5.52; N, 10.96. Found: C, 81.14; H, 5.64; N, 10.85.

Table 1
Crystal data and structure refinement for **6b**.

Empirical formula	$C_{55.50}H_{54}Cl_{4.50}N_6O_2$
Formula weight	996.57
Temperature (K)	110(2) K
Crystal system, space group	Monoclinic, C2/c
Unit cell dimensions	
a (Å)	46.662(6)
b (Å)	9.6597(12)
c (Å)	24.814(3)
α (°)	90.000
β (°)	116.996(2)
γ (°)	90.000
Volume (Å^3)	9966(2)
Z	8
D_{Calc} (Mg/m^3)	1.328
Absorption coefficient (mm^{-1})	0.314
F (0 0 0)	4172
Crystal size (mm)	0.47 × 0.24 × 0.19
θ range for data collection (°)	0.98–26.00
Limiting indices	$57 \le h \le 57$, $-11 \le k \le 7$, $-29 \le l \le 30$
Reflections collected/unique	27 929/9727 [$R_{(int)}$ = 0.0582]
Completeness to theta = 26.00	99.4%
Refinement method	Full-matrix least-squares on F^2
Data/restraints/parameters	9727/0/632
Absorption correction	Semi-empirical from equivalents
Goodness-of-fit on F^2	1.025
Final R indices [$I > 2$sigma(I)]	R_1 = 0.0769, wR_2 = 0.2055
R indices (all data)	R_1 = 0.1425, wR_2 = 0.2639
Largest diff. peak and hole (eÅ^{-3})	0.864 and −1.253
CCDC	738503

Table 2
Selected bond lengths (Å) and angles (°) for **6b**.

Bond lengths			
N(2)–C(49)	1.464(6)	N(3)–C(4)	1.462(5)
C(5)–C(6)	1.467(6)	C(12)–C(13)	1.469(6)
C(19)–C(20)	1.473(6)	C(23)–C(26)	1.460(6)
C(27)–C(28)	1.461(6)	C(31)–C(34)	1.474(6)
C(35)–C(36)	1.473(6)	C(42)–C(43)	1.478(6)
Bond angles			
N(1)–C(34)–C(31)	121.2(4)	N(1)–C(35)–C(36)	119.0(4)
N(2)–C(34)–C(31)	126.9(4)	N(2)–C(42)–C(44)	122.5(4)
N(3)–C(5)–C(6)	125.0(4)	N(3)–C(19)–C(20)	126.3(4)
N(4)–C(12)–C(13)	121.1(4)	N(4)–C(19)–C(20)	123.3(4)
N(5)–C(27)–C(28)	128.2(4)	N(6)–C(26)–C(23)	129.3(4)
O(1)–C(26)–C(23)	118.5(4)	O(1)–C(27)–C(28)	119.2(4)
C(4)–N(3)–C(5)	125.1(3)	C(4)–N(3)–C(19)	127.1(3)
C(5)–C(6)–C(7)	121.8(4)	C(5)–C(6)–C(11)	120.0(4)
C(5)–C(12)–C(13)	128.7(4)	C(6)–C(5)–C(12)	129.5(4)
C(12)–C(13)–C(14)	121.9(4)	C(12)–C(13)–C(18)	119.4(4)
C(19)–C(20)–C(21)	118.2(4)	C(19)–C(20)–C(25)	122.9(4)
C(22)–C(23)–C(26)	119.7(4)	C(24)–C(23)–C(26)	120.7(4)
C(27)–C(28)–C(33)	121.5(4)	C(27)–C(28)–C(29)	118.9(4)
C(30)–C(31)–C(34)	118.1(4)	C(32)–C(31)–C(34)	122.9(4)
C(34)–N(2)–C(49)	126.1(4)	C(35)–C(36)–C(37)	119.3(4)
C(35)–C(36)–C(41)	122.3(4)	C(35)–C(42)–C(43)	131.7(4)
C(42)–C(35)–C(36)	131.3(4)	C(42)–C(43)–C(44)	120.4(4)
C(42)–C(43)–C(48)	121.5(4)	C(42)–N(2)–C(49)	125.5(4)

2.3. Determination of crystal structure of *6b*

The needle-shaped single crystals of **6b** suitable to X-ray structural analysis were obtained by evaporation of 50% ethanol and chloroform solution. The diffraction data for structure was collected with an Bruker Smart 1000 CCD X-ray single crystal diffractometer using a graphite monochromated Mo Kα radiation ($\lambda = 0.71073$ Å) at 110(2) K. The structures were solved by direct methods with SHELXS-97 program and refinements on F^2 were performed with SHELXL-97 program by full-matrix least-squares techniques with anisotropic thermal parameters for the non-hydrogen atoms. All H atoms were initially located in a different Fourier map. A summary of the crystallographic data and structure refinement details is given in Table 1, and the selected bond lengths and angles are presented in Table 2. The crystal structure and cell structure of **6b** are shown in Figs. 4 and 5, respectively.

3. Results and discussion

3.1. Synthesis

Twelve aromatic substituted 1,3,4-oxadiazoles were successfully obtained in 6–23% yields. The key stage in the synthesis of these target molecules is the preparation of **2a**–**c**. Compounds **1a**–**c** possess a larger conjugated-system structure, it is hard for these compounds to be dissolved in most of common solvents, which limits their use as intermediate in synthesis. But the solubility of these compounds for common organic solvents could be improved by introducing some alkyls into the molecules of these compounds.

Many methods were reported for the alkylation of imidazole compounds, several deprotonation reagents, such as sodium, potassium or sodium hydride [37,38], 50% sodium hydroxide in DMF [39], solid potassium hydroxide [40], 1,8-diaza-bicyclo[5,4,0] undec-7-ene [41] were tried in this work. However, theses reported procedures were unsuitable for **1a**–**c**. We ever reported the alkylation reaction of imidazole compounds [30,31], using TBAB as phase-transfer catalyst in butanone and using 50% sodium hydroxide as base. At the beginning of this work, compound **3a** was prepared as the procedure in Fig. 3.

Our group attempted to obtain compound **2a** not using **2d** as intermediate. In this process, a lot of alkylation reaction conditions were tested by varying base reagents, reaction temperature and reaction time. As shown in Fig. 1, this idea eventually could be realized by replacement of 50% NaOH with 50% K_2CO_3 in alkylation reaction shown in Fig. 3.

It is noteworthy that such a procedure for alkylation reaction of imidazole derivatives could be suitable to methyl 4-(4,5-diphenylimidazol-2-yl)benzoate and methyl 4-(phenanthroimidazol-2-yl) benzoate, and this reaction could afford a satisfied yield (70–75%).

3.2. Crystal structure

As can be seen from Fig. 4 and from Table 1, the bond lengths of C5–C6, C12–C13, C19–C20, C23–C26, C27–C28, C31–C34, C35–C36, C42–C43, N3–C4, and N2–C49 are, as expected, shorter than a normal carbon–carbon single bond and nitrogen-carbon single bond due to a conjugation effect. The dihedral angle between the N3/C5/C12/N4/C19 ring and C6/C7/C8/C9/C10/C11 ring is 60.24°, 34.73° for the C13/C14/C15/C16/C17/C18 ring, and 43.10° for C20/C21/C22/C23/C24/C25 ring. The dihedral angle between the N1/C34/N2/C42/C35 ring and C31/C32/C33/C28/C29/C30 ring is 41.55°, 23.72° for the C36/C37/C38/C39/C40/C41 ring, and 86.02° for C43/C44/C45/C46/C47/C48 ring. The dihedral angle between the O1/C26/N6/N5/C27 ring and the C20/C21/C22/C23/C24/C25 ring is 3.19°, and 12.66° for the ring C31/C32/C33/C28/C29/C30. It could be found from all the dihedral data that compound **6b** is not a coplanar molecule.

3.3. Spectral properties

3.3.1. UV–visible absorption spectra

For UV–visible absorption measurements, the dye concentration was 1×10^{-6} M, and the absorption data are summarized in Table 3. The UV–visible absorption spectra of compounds **4g** and **4i** are given as an example in Fig. 6. Several absorption peaks could be observed in the linear absorption spectra of the two molecules in the wavelength range from 237 to 407 nm, while almost no linear absorption was observed beyond 425 nm. It can

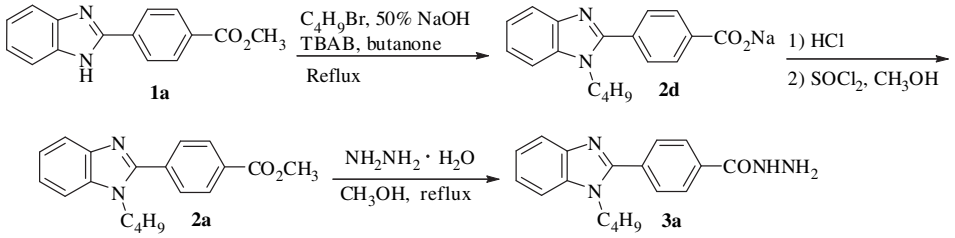

Fig. 3. The synthesis of compound **3a**.

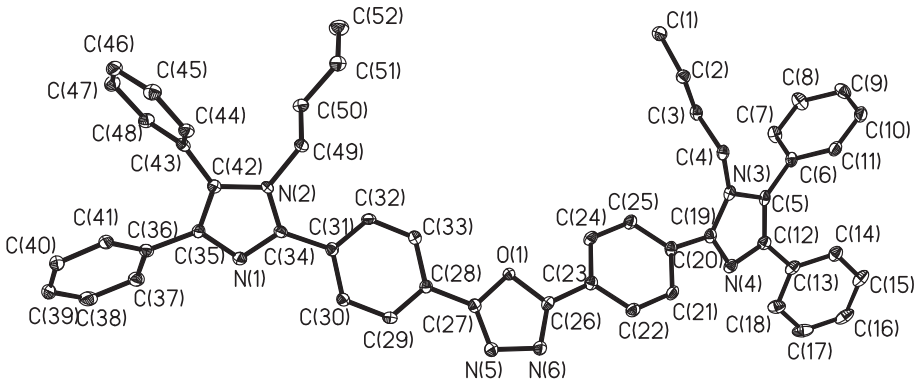

Fig. 4. The molecular structures of **6b**, H atoms and the molecular structures of solvents are omitted for clarity.

be seen that they display very similar absorptions and the strong absorption band at 260 nm, which should originate from the benzene ring and thiophene ring of the molecules. The relatively weak absorption bands between 279 and 407 nm are assigned to the π-π^* electronic transition focusing on the conjugated 1,3,4-oxadiazole, and phenanthroimidazole units.

3.3.2. Fluorescence spectra

The excitation and emission spectra of these compounds were investigated in diluted dichloromethane as well as in the solid state (Tables 3 and 4). The maximum wavelengths of their excitation and emission in dichloromethane are longer than that in solid state, respectively, because the chromophores are completely dispersed in the dilute solution whereas among the chromophores in solid state exist intermolecular associating interactions.

If a comparison is drawn among these compounds in dichloromethane, it can be seen from Table 3 that the excitation spectra and emission spectra slightly shift to the longer wavelength with the increase of conjugated-system. However, for the λ_{ex} and λ_{em} values of compounds **4d**–**i**, there is a consequence: **4e** (359 nm, 445 nm) > **4f** (358 nm, 444 nm) > **4d** (355 nm, 441 nm); **4h** (369 nm, 448 nm) ≈ **4i** (368 nm, 448 nm) > **4g** (367 nm, 446 nm), respectively. This can be attributed to the thiophene ring which possesses a large-radius sulfur atom, which would make the electron-pair on the sulfur atom absorb lower energy to shift into π^* orbit from *n* orbit.

Interestingly, in the solid state, there is a consequence for the λ_{ex} values: **4i** (420 nm) > **4h** (399 nm) > **4g** (394 nm) > **4f** (368 nm) > **4e** (364 nm) > **4d** (361 nm). However, for their λ_{em} values, the order is **4g** (487 nm) > **4i** (478 nm) > **4h** (462 nm) > **4f** (439 nm) > **4d** (430 nm) > **4e** (414 nm). This is due to the stronger intermolecular associating interactions for dyes including thiophene ring, which contains a large-radius sulfur atom.

3.3.3. Fluorescence quantum yields

Fluorescence quantum yields (Φ_F) were determined by a comparative method [42,43] (Equation (1)), using coumarin 1 (purchased from Sigma–Aldrich) as a standard sample with $\Phi_F = 0.99$ in ethyl acetate [44] as the reference.

$$\Phi_F = \Phi_F(S)\frac{F_X \cdot A_S \cdot n_X^2}{F_S \cdot A_X \cdot n_S^2} \quad (1)$$

where F_x and F_S are the areas under the fluorescence emission curves of the sample and standard, respectively. A_x and A_S are the absorbance of the sample and standard, respectively; and n_x and

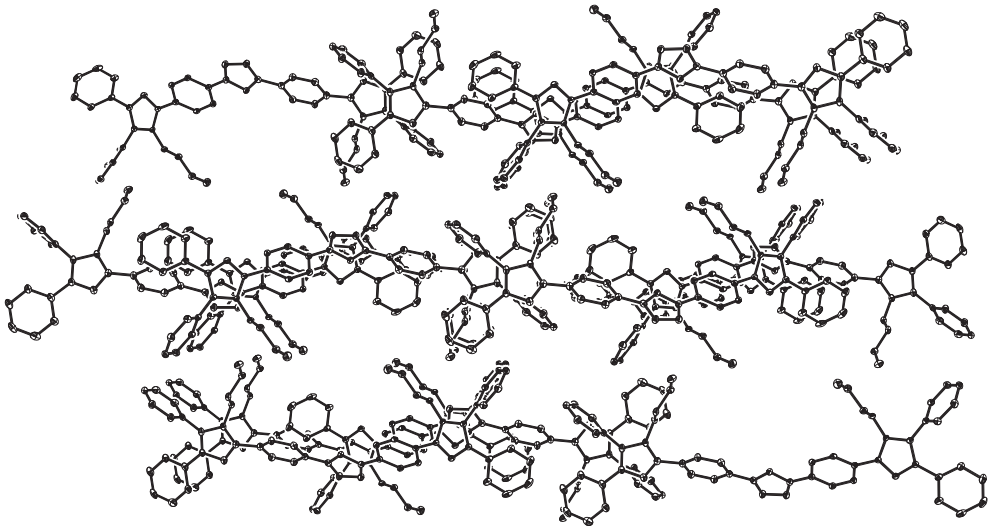

Fig. 5. A packing diagram for **6b**, H atoms and the molecular structures of solvents are omitted for clarity.

Table 3
The λ_{max}, log ε, λ_{ex}, λ_{em}, Stokes shift, Φ_F values, and the lifetime of fluorescence of some samples in dichloromethane.

Sample	λ_{max}/nm (log ε)	λ_{ex}/nm	λ_{em}/nm	Stokes shift/nm	Φ_F	T_1/ns
4d	278 (4.51), 339 (4.43)	355	441	86	0.21	1.76
4e	276 (4.48), 293 (4.37), 311 (4.36), 340 (4.42)	359	445	86	0.62	1.74
4f	294 (4.45), 308 (4.42), 340 (4.50)	358	444	86	0.33	1.65
4g	260 (4.62), 335 (1.56), 363 (1.43)	367	446	81	0.61	1.84
4h	260 (4.87), 308 (4.51), 340 (4.47), 363 (4.41)	369	448	79	0.75	1.78
4i	260 (4.75), 301 (4.43), 341 (4.39), 363 (4.36)	368	448	80	0.62	1.76
6a	331 (4.71)	346	407	61	0.63	0.99
6b	273 (4.51), 352 (4.57)	369	445	76	0.69	1.56
6c	260 (5.06), 347 (4.60), 366 (4.67)	374	451	77	0.78	1.64

n_S are the refractive indices of the solvents used for sample and standard, respectively. Both the sample and the reference were excited at the same wavelength. The absorbance of the solutions at the excitation wavelength ranged between 0.04 and 0.05. [45] The Φ_F values for **4d**, **4e**, **4f**, **4g**, **4h**, **4i**, **6a**, **6b** and **6c** were listed in Table 3.

Concerning the fluorescence quantum yields, the compounds can be obviously divided in two groups. The two-imidazole-substituted compounds (**6a**–**c**) exihited high fluorescence efficiency ($\Phi_F = 0.63$, 0.69, and 0.78, respectively), while the mono-imidazole-substituted compounds (**4d**–**i**) were less emissive. The main reason for high fluorescence quantum yields of these reported compounds is that imidazole structure (1-*n*-butylbenzimidazolyl, 1-*n*-butyl-4,5-diphenylimidazol, and 1-*n*-butylphenanthroimidazolyl) restricts the free rotation between benzene ring and oxadiazole [46,47].

Otherwise, it can be found that the Φ_F values for **6a**–**c** increase with the increase of conjugated-system. Compound **6c** exhibited higher fluorescence efficiency than **6b** because Compound **6c** possesses a larger conjugated-system structure than **6b** does. Actually, this deduction could be confirmed by X-ray diffraction data. The three ring planes: N1/C34/N2/C42/C35 ring, C36/C37/C38/C39/C40/C41 ring, and C43/C44/C45/C46/C47/C48 ring are not coplanar. This occurs to the other three planes: N3/C5/C12/N4/C19 ring, C6/C7/C8/C9/C10/C11 ring, and C20/C21/C22/C23/C24/C25 ring.

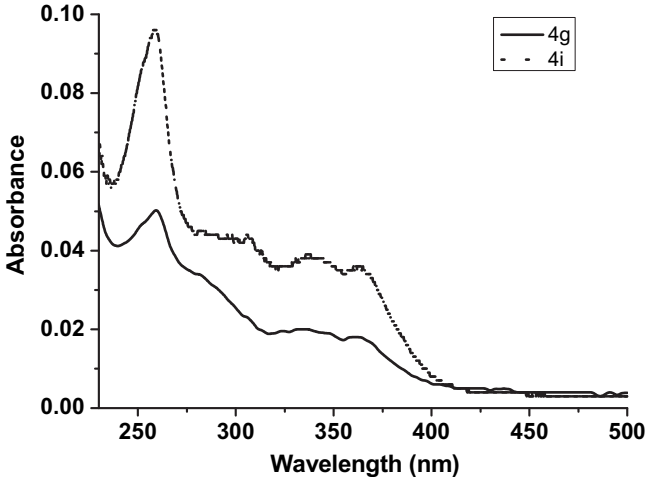

Fig. 6. UV–vis absorption spectra of compounds **4g** and **4i** in dichloromethane.

Table 4
The λ_{ex}, λ_{em}, and the lifetime of fluorescence of some samples in solid sate.

Sample	λ_{ex}/nm	λ_{em}/nm	Stokes shift/nm	T_1/ns (Rel.%)	T_2/ns (Rel.%)
4d	361	430	69	0.83 (87.92)	2.82 (12.08)
4e	364	414	50	0.90 (73.09)	2.89 (26.91)
4f	368	439	71	0.52 (78.25)	1.85 (21.75)
4g	394	487	93	1.09 (75.97)	5.53 (24.03)
4h	399	462	63	0.93 (86.45)	7.39 (13.55)
4i	420	478	58	1.52 (75.21)	5.71 (24.79)
6a	381	442	61	0.65 (83.05)	2.32 (16.95)
6b	415	465	50	0.48 (95.97)	3.55 (4.03)
6c	442	486	44	1.01 (84.63)	6.78 (15.37)

Interestingly, compound **4f** was more emissive than **4d** ($\Phi_F = 0.33$ and 0.21, respectively), and compound **4i** was very similar to **4g** ($\Phi_F = 0.62$ and 0.61, respectively). The reason is also attributed to thiophene ring, which would make the electron-pair in the highest occupied molecular orbit possess a lower energy; the electron-pair could be excited easily to transit into a higher orbit.

3.3.4. Fluorescence lifetimes

The fluorescence lifetime values were determined [48–50] in dichloromethane and in solid state, the obtained data were shown in Tables 3 and 4. T_1 means that lifetime of fluorescence diminished in first-order-progression, T_2 means that lifetime of fluorescence diminished in second-order-progression, and the data in brackets is the ratio of the corresponding decreasing. First-order-progression of samples in dichloromethane was gained. However, both first-order-progression and second-order-progression of samples in solid state were obtained. We could find the following results from Tables 3 and 4:

(1) In solid state, for **4d**–**i** and **6a**–**c**, the T_1 values are all smaller than their corresponding T_2 value.
(2) Comparing the T_1 values of these compounds in dichloromethane with T_1 values of these corresponding compounds in solid state, respectively, we found that the T_1 values in dichloromethane are generally larger than that in solid state.

In addition, some samples showed a shorter fluorescence lifetime in solution and some samples could show a longer fluorescence lifetime in solid state. For example, the lifetime of **6a** is 0.99 ns in dichloromethane, and the T_2 value of **4h** is 7.39 ns in solid state.

3.4. Thermal stability

An organic phosphor applied in the fabricated light-emitting diodes (LEDs) and OLEDs is required to possess a high thermal stability. In order to investigate the thermal stability of the synthesized compounds, the thermogravimetric analysis (TGA) and differential thermogravimetric (DTG) techniques were employed and nine samples (**4d**–**i**, and **6a**–**c**) were measured (see Supporting information), and the decomposition temperature and thermal weightlessness percentage for these nine samples are listed in Table 5.

It could be found from Table 5 that the decomposition temperature for nine samples are all more than 400 °C, and the starting temperature for thermal weightlessness for nine samples is more than 165 °C, which demonstrate that these samples are thermally stable to be used in LEDs and OLEDs.

Table 5
The decomposition temperature and thermal weightlessness percentage for **4d**–**i**, and **6a**–**c**.

Sample	4d	4e	4f	4g	4h	4i	6a	6b	6c
Decomposition temperature (°C)	426.2	462.2	443.3	457.0	474.8	459.6	442.3	479.5	480.9
Weightlessness (%)	6.13	1.87	1.90	20.19	7.77	2.55	1.37	8.39	4.34
Weightlessness temperature (°C)	176.5	251.7	241.3	326.2	319.5	267.7	252.5	301.4	236.7

4. Conclusions

The approach reported here for the alkylation of methyl 4-(benzimidazol-2-yl)benzoate derivatives could be an efficient method, especially for industry, as the reaction condition is mild, the yield is satisfied, solvent could be recycled, the product is easy to be purified.

The procedures reported here could afford an efficient route to introduce imidazole units to 2-position or 5-position of 1,3,4-oxadizole ring, which could provide an attractive and even an efficient approach to the preparation of some useful dyes and pigments.

Herein, 1,3,4-oxadiazole derivatives containing imidazole unit could possess a medium strong fluorescence-emitting ability with Φ_F values in the region of 0.21–0.78. Otherwise, TGA shows that these nine compounds are thermally stable to be used in LEDs and OLEDs. However, it should be pointed out that more experiments must be carried out to estimate their potential application in LEDs and OLEDs.

5. Supplementary material

The crystallographic data (excluding structure factors) of **6b** have been deposited with the Cambridge Crystallographic Center as supplementary publication no. CCDC 738503. Copy of this information may be obtained free of charge via www: http://www.ccdc.cam.ac.ukor from The Director, CCDC, 12 Union Road, Cambridge CB221EZ, UK (fax: +44 1223 336033; email: deposit@ccdc.cam.ac.uk). Structural factors are available on request from the authors.

Acknowledgments

This project is supported by Scientific and Technical Project Foundation of Guangdong Province (2003C103006 and 2007B060401068).

Appendix. Supplementary information

Supplementary data associated with this article can be found, in the online version, at doi:10.1016/j.dyepig.2010.01.011.

References

[1] Pesquet A, Daiech A, Van HL. General and versatile entry to 4,5-fused polycyclic imidazolones systems. Use of the tandem transposition/π-cyclization of *n*-acyliminium Species. Journal of Organic Chemistry 2006;71(14):5303–11.
[2] Bellina F, Cauteruccio S, Montib S, Rossi R. Novel imidazole-based combretastatin A-4 analogues: evaluation of their in vitro antitumor activity and molecular modeling study of their binding to the colchicine site of tubulin. Bioorganic & Medicinal Chemistry Letters 2006;16:5757–62.
[3] Peter W, Wilhelm K. Ionic liquids – new "solutions" for transition metal catalysis. Angewandte Chemie, International Edition 2000;39(21):3772–89.
[4] Zhao Q, Liu SJ, Shi M, Li FY, Jing H, Yi T, et al. Tuning photophysical and electrochemical properties of cationic iridium(III) complex salts with imidazolyl substituents by proton and anions. Organometallics 2007;26:5922–30.
[5] Bellina F, Cauteruccio S, Rossi R. Synthesis and biological activity of vicinal diaryl-substituted ^{1}H-imidazoles. Tetrahedron 2007;63:4571–624.
[6] Park S, Kwon OH, Kim S, Park S, Choi MG, Cha M, et al. Imidazole-based excited-state intramolecular proton-transfer materials: synthesis and amplified spontaneous emission from a large single crystal. Journal of the American Chemical Society 2005;127:10070–4.
[7] Sun YF, Cui YP. The synthesis, structure and spectroscopic properties of novel oxazolone-, pyrazolone- and pyrazoline-containing heterocycle chromophores. Dyes and Pigments 2009;81:27–34.
[8] Shi W, Qian X, Zhang R, Song G. Synthesis and quantitative structure–activity relationships of new 2,5-disubstituted-1,3,4-oxadiazoles. Journal of Agricultural and Food Chemistry 2001;49:124–30.
[9] Chen H, Li Z, Han Y. Synthesis and fungicidal activity against *Rhizoctonia solani* of 2-alkyl (alkylthio)-5-pyrazolyl-1,3,4-oxadiazoles (thiadiazoles). Journal of Agricultural and Food Chemistry 2000;48:5312–5.
[10] Zhou Y, Wang WH, Dou W, Tang XL, Liu WS. Synthesis of a new C2-symmetric chiral catalyst and its application in the catalytic asymmetric borane reduction of prochiral ketones. Chirality 2008;20(2):110–4.
[11] Chochos CL, Govaris GK, Kakali F, Yiannoulis P, Kallitsis JK, Gregoriou VG. Synthesis, optical and morphological characterization of soluble main chain 1,3,4-oxadiazole copolyarylethers-potential candidates for solar cells applications as electron acceptors. Polymer 2005;46:4654–63.
[12] Shang XY, Shu D, Wang SJ, Xiao M, Meng YZ. Fluorene-containing sulfonated poly(arylene ether 1,3,4-oxadiazole) as proton-exchange membrane for PEM fuel cell application. Journal of Membrane Science 2007;291(1+2):140–7.
[13] Pan JF, Zhu WH, Li SF, Zeng WJ, Cao Y, Tian H. Dendron-functionalized perylene diimides with carrier-transporting ability for red luminescent materials. Polymer 2005;46:7658–69.
[14] Zhang XB, Tang BC, Zhang P, Li M, Tian WJ. Synthesis and characterization of 1,3,4-oxadiazole derivatives containing alkoxy chains with different lengths. Journal of Molecular Structure 2007;846:55–64.
[15] Li HL, Kang SS, Xing ZT, Zeng HS, Wang HB. The synthesis, optical properties and X-ray crystal structure of novel 1,3,4-oxadiazole derivatives carrying a thiophene unit. Dyes and Pigments 2009;80:163–7.
[16] Yeh KM, Lee CC, Chen Y. Host copolymers containing pendant carbazole and oxadiazole groups: synthesis, characterization and optoelectronic applications for efficient green phosphorescent OLEDs. Journal of Polymer Science, Part A: Polymer Chemistry 2008;46(15):5180–93.
[17] Huang C, Zhen CG, Su SP, Chen ZK, Liu X, Zou DC, et al. High-efficiency solution processable electrophosphorescent iridium complexes bearing polyphenylphenyl dendron ligands. Journal of Organometallic Chemistry 2009;694(9–10):1317–24.
[18] Zhao DW, Zhang FJ, Xu C, Sun JY, Song SF, Xu Z, et al. Exciplex emission in the blend of two blue luminescent materials. Applied Surface Science 2008;254(11):3548–52.
[19] Froehlich JD, Young R, Nakamura T, Ohmori Y, Li S, Mochizuki A, et al. Synthesis of multi-functional POSS emitters for OLED applications. Chemistry of Materials 2007;19(20):4991–7.
[20] Ahn JH, Wang CS, Perepichka IF, Bryce MR, Petty MC. Blue organic light emitting devices with improved color purity and efficiency through blending of poly(9,9-dioctyl-2,7-fluorene) with an electron transporting material. Journal of Materials Chemistry 2007;17(29):2996–3001.
[21] Lee JH, Tsai HH, Leung MK, Yang CC, Chao CC. Phosphorescent organic light-emitting device with an ambipolar oxadiazole host. Applied Physics Letters 2007;90(24):243501/1–243501/3.
[22] Zhao DW, Song SF, Zhang FJ, Zhao SL, Xu C, Xu Z. The effect of multilayer quantum well structure on the characteristics of OLEDs. Displays 2007;28(2):81–4.
[23] Wolarz E, Chrzumnicka E, Fischer T, Stumpe J. Orientational properties of 1,3,4-oxadiazoles in liquid-crystalline materials determined by electronic absorption and fluorescence measurements. Dyes and Pigments 2007;75(3):753–60.
[24] Zhao DW, Xu Z, Zhang FJ, Song SF, Zhao SL, Wang Y, et al. The effect of electric field strength on electroplex emission at the interface of NPB/PBD organic light-emitting diodes. Applied Surface Science 2007;253(8):4025–8.
[25] Leung MK, Yang CC, Lee JH, Tsai HH, Lin CF, Huang CY, et al. The unusual electrochemical and photophysical behavior of 2,2′-bis(1,3, 4-oxadiazol-2-yl) biphenyls, effective electron transport hosts for phosphorescent organic light emitting diodes. Organic Letters 2007;9(2):235–8.
[26] Su Z, Xie YG, Li X, Yu T. Organic light-emitting devices with a 2-(4-biphenyl)-5-(4-butylphenyl)-1,3,4-oxadiazole layer between the a naphtylphenyliphenyl diamine and 8-hydroxyquinoline aluminum. Microelectronics Journal 2006;37(8):714–7.
[27] Maekawa Y, Kitano Y, Kusabiraki M. Effects of PEDOT-PSS layer on the characteristics of organic light-emitting diodes with Nile Red. e-Journal of Surface Science and Nanotechnology 2005;3:341–4.
[28] Zhu WH, Yao R, Tian H. Synthesis of novel electro-transporting emitting compounds. Dyes and Pigments 2002;54:147–54.
[29] Pan WL, Song JG, Yu WJ, Chen Y, Wan YQ, Song HC. One-step synthesis of 2-benzimidazolyl alkene under microwave irradiation. Acta Scientiarum Naturalium Universitis Sunyatseni 2006;45(6):58–61.
[30] Pan WL, Tan HB, Chen Y, Mu DH, Liu HB, Wan YQ, et al. The synthesis and preliminary optical study of 1-alkyl-2,4,5-triphenylimidazole derivatives. Dyes and Pigments 2008;76:17–23.

[31] Yan YN, Lin DY, Pan WL, Li XL, Wan YQ, Mai YL, et al. Synthesis and optical behaviors of 2-(9-phenanthrenyl)-, 2-(9-anthryl)-, and 2-(1-pyrenyl)-1-alkylimidazole homologues. Spectrochimica Acta Part A: Molecular and Biomolecular Spectroscopy 2009;74:233–42.
[32] Tang HJ, Tang H, Zhang ZG, Yuan JB, Cong CJ, Zhang KL. Synthesis, photoluminescent and electroluminescent properties of a novel europium(III) complex involving both hole- and electron-transporting functional groups. Synthetic Metals 2009;159:72–7.
[33] Henary MM, Wu YG, Cody J, Sumalekshmy S, Li J, Mandal S, et al. Excited-state intramolecular proton transfer in 2-(2′-arylsulfonamidophenyl) benzimidazole derivatives: the effect of donor and acceptor substituents. Journal of Organic Chemistry 2007;72(13):4784–97.
[34] Bu L, Sawada T, Shosenji H, Yoshida K, Mataka S. Crystallographic structures and solid fluorescence behaviors of crystals of a 2-(9-anthryl) phenanthroimidazole-type clathrate host. Dyes and Pigments 2003;57:181–95.
[35] Perry RJ, Wilson BD. A novel palladium-catalyzed synthesis of 2-arylbenzimidazoles. Journal of Organic Chemistry 1993;58:7016–21.
[36] Mohammadi AA, Mivechi M, Kefayati H. Potassium aluminum sulfate (alum): an efficient catalyst for the one-pot synthesis of trisubstituted imidazoles. Monatshefte Für Chemie 2008;139:935–7.
[37] Su CY, Kang BS, Du CX, Yang QC, Mak TCW. Formation of mono-, bi-, tri-, and tetranuclear Ag(I) complexes of C_3-symmetric tripodal benzimidazole ligands. Inorganic Chemistry 2000;39(21):4843–9.
[38] Ghosh S, Nanda KK, Addison AW, Butcher RJ. Mononuclear and mixed-valence binuclear oxovanadium complexes with benzimidazole-derived chelating agents. Inorganic Chemistry 2002;41(8):2243–9.
[39] Lombardino JG. DE 2 155 558; 1972 [US 3 772 441; 1973].
[40] Su CY, Cai YP, Chen CL, Smith MD, Kaim W, Loye HC. Ligand-directed molecular architectures: self-assembly of two-dimensional rectangular metallacycles and three-dimensional trigonal or tetragonal prisms. Journal of the American Chemical Society 2003;125(28):8595–614.
[41] Youngblood WJ. Synthesis of a New *trans*-A_2B_2 phthalocyanine motif as a building block for rodlike phthalocyanine polymers. Journal of Organic Chemistry 2006;71:3345–56.
[42] Parker CA, Rees WT. Correction of fluorescence spectra and measurement of. fluorescence quantum efficiency. Analyst 1960;85:587–600.
[43] Demas JN, Crosby GA. Measurement of photoluminescence quantum yields. Journal of Physical Chemistry 1971;75:991–1024.
[44] Jones II G, Jackson WR, Choi CY, Bergmark WR. Solvent effects on emission yield and lifetime for coumarin laser dyes. Requirements for a rotatory decay mechanism. Journal of Physical Chemistry 1985;89(2):294–300.
[45] Durmuş M, Erdoğmuş A, Ogunsipe A, Nyokong T. The synthesis and photophysicochemical behaviour of novel water-soluble cationic indium(III) phthalocyanine. Dyes and Pigments 2009;82:244–50.
[46] Fakhfakh M, Turki H, Fery-Forgues S, Gharbi RE. The synthesis and optical properties of novel fluorescent iminocoumarins and bis-iminocoumarins: investigations in the series of urea derivatives. Dyes and Pigments 2010;84:108–13.
[47] Tao Y, Xu Q, Lu J, Yang X. The synthesis, electrochemical and fluorescent properties of monomers and polymers containing 2,5-diphenyl-1,3,4-thiadiazole. Dyes and Pigments 2010;84:153–8.
[48] Fang Y. Shi jian fen bian (yingguang) ge xiang yi xing ji qi zai gao fen zi kexue zhong de ying yong. Photographic Science and Photochemistry 1998;16:274–88.
[49] Lakowicaz JR. Principle of fluorescence spectroscopy. 2nd ed. , New York: Academic Plenum Press; 1999.
[50] Ware WR, Doemeny LJ, Nemzek TL. Deconvolution of fluorescence and phosphorescence decay curves. Least-squares method. Journal of Physical Chemistry 1973;77(17):2038–42.